Acta Cryst. (1989). A**45**, 524–533

Structure Factors for Icosahedral Quasicrystals

BY PETER KRAMER AND DIETER ZEIDLER

Institut für Theoretische Physik der Universität Tübingen, Auf der Morgenstelle 14, *D*-7400 *Tübingen, Federal Republic of Germany*

(*Received* 15 *September* 1988; *accepted* 27 *February* 1989)

Abstract

The restriction of a hypercubic lattice in six dimensions to a subspace of three dimensions yields a well known quasiperiodic description of quasicrystals with non-crystallographic icosahedral point symmetry. A quasicrystal model is considered where this description is further reduced to a non-periodic quasilattice formed from two types of rhombohedra. Given the density on two representative rhombohedral cells, the full Fourier transform is expressed in closed form through structure factors, quasilattice factors and kinematical factors. The diffraction from point scatterers in the quasilattice is computed as an example.

1. Introduction

Crystallography in three-dimensional space E^3 uses the concept of a unit cell, its possible point symmetry, and its periodic repetition under translations. Given the atomic density $f(\mathbf{x})$ in position or $\mathbf{x}$-space on the unit cell, the structure factor is essentially its Fourier transform $\tilde{f}(\mathbf{k})$ in $\mathbf{k}$-space. The Fourier transform of the full periodic density, which determines the diffraction pattern, is then the product of the structure factor $\tilde{f}(\mathbf{k})$ with the Fourier transform of the lattice which, due to the periodicity, selects in $\mathbf{k}$-space the discrete set of reciprocal-lattice points which we denote by $\mathbf{k}^R$.

Quasicrystals, in particular those with non-crystallographic point symmetry, lack periodicity but have their Fourier transform still on a discrete set of points in $\mathbf{k}$-space. The corresponding class of functions is in $\mathbf{x}$-space characterized by almost or quasiperiodicity (*cf.* Bohr, 1925*a*, *b*, 1926). Among this class of quasiperiodic functions there exists a class characterized by a non-periodic cell structure. The cells of this class appear as building blocks of a non-periodic quasilattice. The structures of this class have been called quasicrystal models by Kramer (1988).

In the present paper we consider the particular icosahedral quasilattice derived from a hypercubic lattice in E^6. Its cells are two types of rhombohedra (*cf.* Mackay, 1982; Kramer & Neri, 1984). As shown by Kramer (1988), these two rhombohedra serve as quasicrystal cells of the corresponding quasilattice. The Fourier transform admits a factorization into structure factors and factors from the quasilattice. Explicit and closed expressions are given for the Fourier transform. To illustrate the results to be expected from quasicrystal models, the diffraction is computed for point scatterers in the quasilattice.

2. The icosahedral and hyperoctahedral point groups

The icosahedral group I of order 60 may be defined abstractly by its generators g_m, $m = 5, 3, 2$ and by relations between them (Coxeter & Moser, 1965). The crystallographic aspects of this group are better described by its action on Euclidean space E^3 of dimension 3. The well known stereographic projection of the six fivefold, the ten threefold and the 15 twofold axes (Hahn & Klapper, 1983) is displayed in Fig. 1. Moreover the three sets of axes have been labelled by numbers, and by a bar in cases where the vectors associated with a right-hand rotation point downward.

The three rotation axes labelled no. 1 we choose as the generators g_5, g_3 and g_2. The twofold axis no. 15 is perpendicular to all these axes; we denote its generator by g_2'.

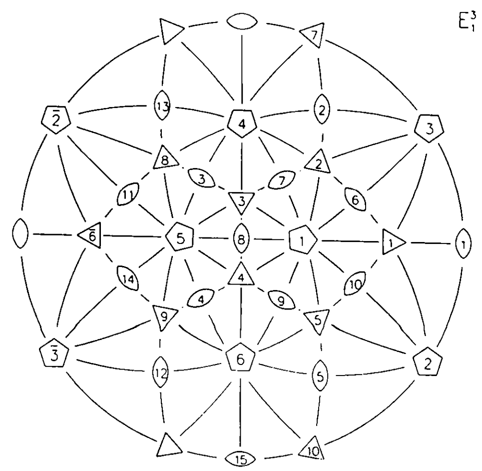

Fig. 1. Stereographic projection of icosahedral symmetry operations in E^3_1. The fivefold axis labelled i corresponds to the projection of the hypercubic basis vector $\mathbf{b}_i$ onto E^3_1. For the labels of the threefold and twofold axes see proposition 2.2. For the coordinate description of the symmetry operations given in Table 4 we use orthogonal axes corresponding to the directions of the twofold axes 15, 1 and 8 respectively.

0108-7673/89/080524-10$03.00

Table 1. *The icosahedral group I, its dihedral subgroups and their coset generators*

Subgroup	Generators	Coset generators	
D_5	g_5, g_2'	$c_i' = (g_5)^\alpha (g_3)^\gamma$,	$i = \alpha + \gamma + 1$
		$\alpha = 0, \dots, 4;\quad \gamma = 0, 1$	$1 \le i \le 6$
		$\alpha \ge 1 \to \gamma = 1$	
D_3	g_3, g_2'	$c_i = (g_5)^\alpha (g_2)^\beta$	$i = \alpha + \beta + 1$
		$\alpha = 0, \dots, 4;\quad \beta = 0, 1$	$1 \le i \le 10$
D_2	g_2, g_2'	$c_i'' = (g_5)^\alpha (g_2)^\beta (g_3)^\gamma$	$i = \alpha + 5(\beta + \gamma) + 1$
		$\alpha = 0, \dots, 4;\quad \beta = 0, 1$	$1 \le i \le 15$
		$\gamma = 0, 1;\quad \beta \le \gamma$	

2.1. *Definition*

The dihedral subgroups D_m generated by g_m and g_2' for $m = 5, 3, 2$ we denote by D_5, D_3 and D_2.

Consider the left cosets I/D_m of the icosahedral group with respect to a dihedral subgroup D_m. By

$$c_i, \qquad i = 1, \dots, 60/(2m) \tag{2.1}$$

we denote sets of generators for the coset I/D_m. An explicit choice is given in Table 1. Different dihedral subgroups are distinguished by primes.

The group elements corresponding to fivefold, threefold and twofold axes are conjugate respectively within I. Each axis may be associated with a dihedral group conjugate to one of the three subgroups described in definition 2.1. Since there is no other group element in I which commutes with a given dihedral subgroup, one gets:

2.2. *Proposition*

The left coset generators c_i by the conjugation map

$$\varphi_i\colon D_m \to c_i D_m c_i^{-1}, \qquad i = 1, \dots, 60/(2m) \tag{2.2}$$

generate the dihedral groups associated with the axes of I.

Through this correspondence, the index i of a coset generator labels the axes of the icosahedral group. With the choice

$$c_1 = e, \tag{2.3}$$

these labels appear in Table 1 and are used in Fig. 1 to enumerate the axes.

The action of I on E^3 used so far corresponds in representation theory to one of the two three-dimensional irreducible representations of I, denoted by $[31^2_+]$ by Haase, Kramer, Kramer & Lalvani (1987). The two three-dimensional representations appear in the explicitly reduced form of a six-dimensional representation. The matrices of the generators for these representations are given by Kramer (1987). The six-dimensional representation is technically obtained as a representation of I induced from a one-dimensional representation of D_5 (Haase *et al.*, 1987).

For the present purpose this six-dimensional construction may be obtained in a non-technical fashion as follows: Any element g of I corresponds to a rotation associated with one of the axes shown in Fig. 1. The action of g on E^3 must transform the set of six fivefold rotation axes into themselves and hence may be described by a signed permutation of the numbers $1, \dots, 6$. A sign $\varepsilon = \pm 1$ indicates if an axis is to be reversed under g. For the generators, these signed permutations are given in Table 2. We use the shorthand notation

$$(\varepsilon, p) \to \begin{bmatrix} 1 & \dots & 6 \\ \varepsilon_1 p(1) & \dots & \varepsilon_6 p(6) \end{bmatrix}. \tag{2.4}$$

Table 2. *The generators of the icosahedral group as elements of the hyperoctahedral group $\Omega(6)$ in the notation of equation* (2.4)

Group element	Permutation matrix
g_5	$\begin{bmatrix} 1 & 2 & 3 & 4 & 5 & 6 \\ 1 & 3 & 4 & 5 & 6 & 2 \end{bmatrix}$
g_3	$\begin{bmatrix} 1 & 2 & 3 & 4 & 5 & 6 \\ 2 & 3 & 1 & 6 & -4 & -5 \end{bmatrix}$
g_2	$\begin{bmatrix} 1 & 2 & 3 & 4 & 5 & 6 \\ -5 & 3 & 2 & -4 & -1 & -6 \end{bmatrix}$
g_2'	$\begin{bmatrix} 1 & 2 & 3 & 4 & 5 & 6 \\ -1 & -3 & -2 & -6 & -5 & -4 \end{bmatrix}$

Multiplication of group elements clearly yields a homomorphism. Once the permutations are represented by 6×6 permutation matrices, this leads to an embedding into the hyperoctahedral point group $\Omega(6)$ (Kramer & Haase, 1988):

2.3. *Definition*

The defining representation for an element (ε, p) of the hyperoctahedral group $\Omega(n)$ is the product of an $n \times n$ diagonal reflection matrix ε and an $n \times n$ permutation matrix associated with p,

$$D_{ij}(\varepsilon, p) = \varepsilon_i \delta_{i, p(j)}. \tag{2.5}$$

The hyperoctahedral group consists of all these elements and has the order

$$|\Omega(n)| = n!2^n. \tag{2.6}$$

It is the point group of the symmorphic hypercubic space group which we denote as $(T, \Omega(n))$, with T being the hypercubic translation group.

From the six-dimensional construction given above, one finds:

2.4. *Proposition*

The icosahedral group I is a subgroup of the hyperoctahedral point group $\Omega(6)$ and hence of the hypercubic space group.

The six-dimensional representation of I is reducible. Its explicit reduction into the representations $[31^2_+]$ and $[31^2_-]$ is obtained by transforming with the 6×6 matrix M given in Table 3 which is adapted to the present notation from Kramer (1987). The matrix

Table 3. *The reducing matrix M*

The ith column of the matrix M corresponds to the ith basis vector of the hypercubic lattice. The three top and bottom rows determine the projections of these vectors onto the subspaces E_1^3 and E_2^3. We use $s=\sin\beta$, $c=\cos\beta$, $\tan\beta=\Phi^{-1}$, $\beta=31{\cdot}717°$, $\Phi=(1+\sqrt{5})/2$.

$$M=\sqrt{\tfrac{1}{2}}\begin{bmatrix} 0 & s & -s & -c & 0 & c \\ s & c & c & 0 & -s & 0 \\ c & 0 & 0 & s & c & s \\ 0 & c & -c & s & 0 & -s \\ c & -s & -s & 0 & -c & 0 \\ -s & 0 & 0 & c & -s & c \end{bmatrix}$$

M yields an orthogonal subspace decomposition

$$E^6 \to E_1^3 + E_2^3. \tag{2.7}$$

In E_1^3, the action of I is the one discussed before and illustrated in Fig. 1. In Fig. 2 the elements of I are described in a similar fashion as in Fig. 1, but for the second three-dimensional subspace E_2^3. In E_2^3, the action of I and of its generators are again described by the permutations given in Table 2. If one chooses orthonormal systems of coordinates as indicated in the captions to Figs. 1 and 2, the action of the generators may also be described by 3×3 rotation matrices given in Table 4. It can be seen that, for example, the element g_5 corresponds in E_2^3 to a rotation by $4\pi/5$ (*cf.* Fig. 2).

3. The hypercubic cell complex in E^6, its dual and its *Klötze*

The hypercubic lattice in E^6 has as its basis an orthonormal set of vectors $\mathbf{b}_i$, $i=1,\ldots,6$. Its unit cell

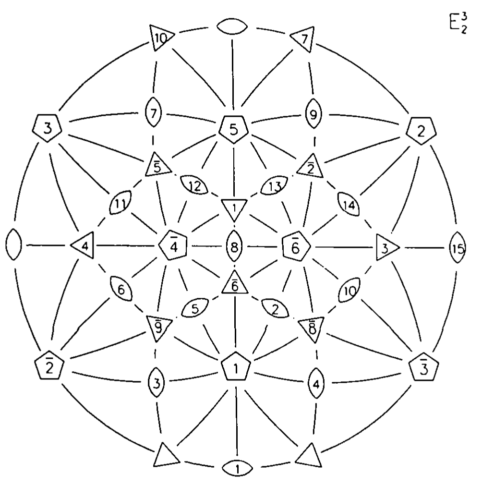

Fig. 2. Stereographic projection of icosahedral symmetry operations in E_2^3. The fivefold axis labelled i corresponds to the projection of the hypercubic basis vector $\mathbf{b}_i$ onto E_2^3. For the labels of the threefold and twofold axes see proposition 2.2. For the coordinate description of the symmetry operations given in Table 4 we use orthogonal axes corresponding to the directions of the twofold axes 1, 15 and 8 respectively.

Table 4. *The irreducible representation* $[31_+^2]$ *and* $[31_-^2]$ *for the generators of the icosahedral group in* E_1^3 *and* E_2^3 *respectively*

For reasons of simplicity the generator $g_3'=c_5g_3c_5^{-1}$ is given instead of g_3; compare Figs. 1, 2.

Group element	Representation $[31_+^2]$	Representation $[31_-^2]$
g_5	$\frac{1}{2}\begin{bmatrix} \Phi^{-1} & -\Phi & 1 \\ \Phi & 1 & \Phi^{-1} \\ -1 & \Phi^{-1} & \Phi \end{bmatrix}$	$\frac{1}{2}\begin{bmatrix} -\Phi & \Phi^{-1} & 1 \\ -\Phi^{-1} & 1 & -\Phi \\ -1 & -\Phi & -\Phi^{-1} \end{bmatrix}$
g_3'	$\begin{bmatrix} 0 & 0 & 1 \\ 1 & 0 & 0 \\ 0 & 1 & 0 \end{bmatrix}$	$\begin{bmatrix} 0 & 0 & 1 \\ 1 & 0 & 0 \\ 0 & 1 & 0 \end{bmatrix}$
g_2	$\begin{bmatrix} -1 & 0 & 0 \\ 0 & 1 & 0 \\ 0 & 0 & -1 \end{bmatrix}$	$\begin{bmatrix} -1 & 0 & 0 \\ 0 & 1 & 0 \\ 0 & 0 & -1 \end{bmatrix}$
g_2'	$\begin{bmatrix} 1 & 0 & 0 \\ 0 & -1 & 0 \\ 0 & 0 & -1 \end{bmatrix}$	$\begin{bmatrix} 1 & 0 & 0 \\ 0 & -1 & 0 \\ 0 & 0 & -1 \end{bmatrix}$

is the hypercube

$$h(6)=\{\mathbf{y}\,|\,-\tfrac{1}{2}\le \mathbf{y}\,.\,\mathbf{b}_i\le\tfrac{1}{2},\ i=1,\ldots,6\}. \tag{3.1}$$

For reasons of simplicity we have chosen $|\mathbf{b}_i|=1$, hence the volume of the unit cell is 1. Its boundaries of dimension p, called p-boundaries in what follows, may be characterized by:

3.1. *Definition*

Let $g=(\varepsilon, r)$ denote a general element of the hyperoctahedral group $\Omega(6)$. The corresponding p-boundary is the set of points

$$h(p;g)=\left\{\mathbf{y}\,|\,\mathbf{y}=\tfrac{1}{2}\sum_{j=p+1}^{6}\varepsilon_{r(j)}\mathbf{b}_{r(j)} + \tfrac{1}{2}\sum_{i=1}^{p}\varepsilon_{r(i)}\lambda_{r(i)}\mathbf{b}_{r(i)},\ -1\le\lambda_j\le 1\right\} \tag{3.2}$$

where empty sums are defined to be zero.

The stability subgroup of $\Omega(6)$ which transforms a p-boundary into itself is conjugate to the group $S(6-p)\times\Omega(p)$, and from the dimensions of the groups the number of p-boundaries is

$$\nu(p)=\binom{6}{p}\,.\,2^{6-p}. \tag{3.3}$$

Let the translation group T act on the hypercubic cell and on its boundaries. The corresponding geometric object in E^6 we call the *hypercubic cell complex Y*. If we restrict this object to all boundaries of dimension up to p, we call it the *p-skeleton* $Y^{(p)}$ of Y. These notions are derived from algebraic topology (Munkres, 1984). Now we pass to a geometric object in E^6 which will be called the *metrical dual* Y^*.

3.2. *Definition*

The metrical dual boundary to a p-boundary is the set of points in E^6:

$$h^*(6-p;g)=\left\{\mathbf{y}\,|\,\mathbf{y}=\tfrac{1}{2}\sum_{j=p+1}^{6}\varepsilon_{r(j)}\mathbf{b}_{r(j)}+\tfrac{1}{2}\sum_{j=p+1}^{6}\varepsilon_{r(j)}\lambda_{r(j)}\mathbf{b}_{r(j)}\right\}. \quad (3.4)$$

The $(6-p)$-boundary $h^*(6-p;g)$ and the p-boundary $h(p;g)$ intersect in a single point, have complementary dimension and are spanned, with respect to this point, by mutually orthogonal sets of vectors. We include $h^*(0)=0$.

If the translation group T acts on all dual boundaries, it generates a geometric object which we term the *metrical dual cell complex* Y^*. From definition 3.2, it is not hard to see that Y^* has precisely the same intrinsic geometric structure as Y, but is shifted with respect to Y by the vector from the midpoint to a vertex of the first hypercube. This simplicity of the dual is a special feature of hypercubic lattices and does not generalize to other lattices (Kramer, 1989).

Consider now a subspace decomposition of E^6 of the form

$$E^6\to E_1^3+E_2^3. \quad (3.5)$$

By the subscripts 1 and 2 we shall denote the orthogonal projections of vectors and of polytopes into these subspaces.

3.3. *Definition*

Let $Y^{(3)}$ and $Y^{*(3)}$ denote the 3-skeletons of Y and Y^*. To a pair of metrical dual boundaries $h(3;g)$ and $h^*(3;g)$ associate the *Klotz* as the six-dimensional polytope

$$kl(3+3;g)=\{\mathbf{y}\,|\,\mathbf{y}=\mathbf{y}_1+\mathbf{y}_2,\mathbf{y}_2\in h_2(3;g),\mathbf{y}_1\in h_1^*(3;g)\}. \quad (3.6)$$

The two projections of a *Klotz* to the spaces E_1^3 and E_2^3 we term its 1-*chart* and its 2-*chart*.

The projections of 3-boundaries to the subspaces E_1^3 and E_2^3 which form these charts have a simple interpretation: Given the three basis vectors which span the corresponding boundary, one finds the projections of these vectors in E_1^3 and E_2^3 as the vectors along the fivefold rotation axes in Figs. 1 and 2 with the labels corresponding to the three indices of the basis vectors. The projected boundaries are the rhombohedra spanned by these vectors. In particular the projections $h_1^*(3;g)$ are rhombohedra with one vertex at the point $\mathbf{y}=0$. These projections appear in two shapes, a thin and a thick rhombohedron. Both polyhedra have point stability groups D_3 with respect to their centres, and each one can appear in ten possible orientations. This means that from two representatives, a thin and a thick rhombohedron, one can generate by icosahedral rotations all orientations and by translation vectors projected to the subspace all positions. We shall choose the representatives so that the dihedral group D_3 specified in Table 1 becomes the stability group of these two rhombohedra. We denote these two representatives by kl_α and kl_β. The group elements g_α, g_β for these two representatives are defined as

$$kl_\xi=kl(3+3;g_\xi)=\{\mathbf{y}\,|\,\mathbf{y}=\mathbf{y}_1+\mathbf{y}_2,\mathbf{y}_2\in h_2(3;g_\xi),\mathbf{y}_1\in h_1^*(3;g_\xi)\}\qquad \xi=\alpha,\beta \quad (3.7)$$

where from (3.2) and (3.4)

$\xi=\alpha$:

$$\begin{aligned}h(3;g_\alpha)&=\{\mathbf{y}\,|\,\mathbf{y}=\tfrac{1}{2}(-\mathbf{b}_5+\mathbf{b}_4+\mathbf{b}_6)+\tfrac{1}{2}(\lambda_1\mathbf{b}_1+\lambda_2\mathbf{b}_2+\lambda_3\mathbf{b}_3)\}\\ h^*(3;g_\alpha)&=\{\mathbf{y}\,|\,\mathbf{y}=\tfrac{1}{2}(-\mathbf{b}_5+\mathbf{b}_4+\mathbf{b}_6)+\tfrac{1}{2}(-\lambda_5\mathbf{b}_5+\lambda_4\mathbf{b}_4+\lambda_6\mathbf{b}_6)\},\end{aligned} \quad (3.8)$$

$\xi=\beta$:

$$\begin{aligned}h(3;g_\beta)&=\{\mathbf{y}\,|\,\mathbf{y}=\tfrac{1}{2}(\mathbf{b}_1+\mathbf{b}_2+\mathbf{b}_3)+\tfrac{1}{2}(-\lambda_5\mathbf{b}_5+\lambda_4\mathbf{b}_4+\lambda_6\mathbf{b}_6)\}\\ h^*(3;g_\beta)&=\{\mathbf{y}\,|\,\mathbf{y}=\tfrac{1}{2}(\mathbf{b}_1+\mathbf{b}_2+\mathbf{b}_3)+\tfrac{1}{2}(\lambda_1\mathbf{b}_1+\lambda_2\mathbf{b}_2+\lambda_3\mathbf{b}_3)\}.\end{aligned} \quad (3.9)$$

From Fig. 1 it is easy to see that the 1-charts $h_1^*(3;g_\alpha)$ and $h_1^*(3;g_\beta)$ span a thin or a thick rhombohedron respectively whose threefold symmetry axis has the number 1. By acting with the coset representatives of I/D_3 on these two rhombohedra, one obtains a total of 20 rhombohedra. These 20 rhombohedra will play a fundamental role in the quasicrystal model.

We now summarize the main results of the six-dimensional analysis given by Kramer (1988), in the notation of § 2. Consider the two *Klötze* called kl_α and kl_β specified in (3.7)–(3.9) and their images in E^6 under the coset generators of I/D_3. These 20 six-dimensional polyhedra form a new *fundamental domain* (FD) for the hypercubic lattice in E^6. The translated copies of these 20 *Klötze* provide a *periodic space filling* of E^6. This means that a six-dimensional density could be supported on this collection of *Klötze*.

With these results, one can describe a *quasilattice* in E_1^3 as follows. Consider a subspace E_1^3 in E^6 which contains the point $\mathbf{c}_2$. This subspace will intersect with the *Klötze* of the periodic space filling, and its intersection with a given *Klotz* will be its 1-chart, that is, a thin or a thick rhombohedron. These rhombohedra appear in face-to-face position, and they fill E_1^3 non-periodically since, by construction, there can be no translation vector within E_1^3. This discrete

Table 5. *Elements g of the hyperoctahedral group $\Omega(6)$ which determine the representatives for $p = 3$, 4, 5*

$$p=3 \quad g_\alpha = \begin{bmatrix} 1 & 2 & 3 & 4 & 5 & 6 \\ 1 & 2 & 3 & -5 & 4 & 6 \end{bmatrix} \quad \text{thin rhombohedron in } E_1^3$$

$$p=3 \quad g_\beta = \begin{bmatrix} 1 & 2 & 3 & 4 & 5 & 6 \\ -5 & 4 & 6 & 1 & 2 & 3 \end{bmatrix} \quad \text{thick rhombohedron in } E_1^3$$

$$p=4 \quad g_\gamma = \begin{bmatrix} 1 & 2 & 3 & 4 & 5 & 6 \\ 3 & 2 & -5 & -6 & 4 & 1 \end{bmatrix}$$

$$p=5 \quad g_\delta = \begin{bmatrix} 1 & 2 & 3 & 4 & 5 & 6 \\ 1 & 4 & 5 & 6 & 2 & 3 \end{bmatrix}$$

non-periodic geometric object formed from rhombohedra will be called the quasilattice.

The boundaries of the representative quasicrystal cells are the faces, edges and vertices of rhombohedra described by the projections $h_1^*(6-p; g)$, $p = 4$, 5, 6. In E^6 they correspond to boundaries of dimension $(6-p)+3$ with 2-charts of the form $h_2(3; \tilde{g})$. A representative *Klotz* boundary for fixed p is found by fixing a 1-chart $h_1^*(6-p; g)$ and collecting all 2-charts $h_2(3; \tilde{g})$ which have points on this boundary. These representative *Klotz* boundaries were found in Kramer (1988) and have the form of new types of *Klötze*

$$kl((6-p)+3; g)$$
$$= \{\mathbf{y} \,|\, \mathbf{y} = \mathbf{y}_1 + \mathbf{y}_2, \mathbf{y}_2 \in h_2(p; g), \mathbf{y}_1 \in h_1^*(6-p; g)\},$$
$$p = 4, 5, 6. \quad (3.10)$$

For the choices $g = g_\xi$ given in Table 5, the representative *Klotz* boundaries are stable for $p = 4$, 5, 6 under the point groups $St = D_2$, D_5 and I respectively. A full representative set with respect to the pure translation group is obtained by acting with the generators of the cosets I/St. If the density is concentrated on these boundaries and if the quasicrystal model is considered, then this density will be given as a function on the points of $h_1^*(6-p; g)$, independent of the points of $h_2(p; g)$.

The *quasicrystal model* considered in what follows is obtained by restricting the six-dimensional density so that on each *Klotz* it becomes independent of the coordinate $\mathbf{x}_2$ perpendicular to E_1^3. As a consequence, this density is essentially supported on the 1-chart of the 20 representative *Klötze*. If moreover we assume the icosahedral point symmetry, this density must have D_3 symmetry on each rhombohedron, and it must be fixed to this rhombohedron independent of its orientation. In this quasicrystal model, the rhombohedral cells of the quasilattice described above play a role similar to the unit cells of periodic order.

4. Fourier transform, structure factors and kinematical factors

Consider the six-dimensional $\mathbf{k}$-space and the reciprocal lattice Y^R with the reciprocal translation group T^R. Clearly Y^R is again a hypercubic lattice. We introduce in $\mathbf{k}$-space the same decomposition

$$E^6 \to E_1^3 + E_2^3 \quad (4.1)$$

as in $\mathbf{x}$-space and denote the projections of vectors in $\mathbf{k}$-space again by the subscripts 1, 2. For the Fourier transform we start from:

4.1. *Proposition*

Let $f(\mathbf{y}_1, \mathbf{y}_2)$ denote the periodic density in E^6 on the hypercubic lattice, expressed in coordinates parallel and perpendicular to the subspace E_1^3, and let

$$f(\mathbf{y}_1) = f(\mathbf{y}_1, \mathbf{y}_2)|_{\mathbf{y}_2 = \mathbf{c}_2} \quad (4.2)$$

be its restriction to E_1^3. Then the Fourier transform of this density, taken as a function on E_1^3, is given by

$$\tilde{f}(\mathbf{k}_1) = [\mathrm{vol.}\,(\mathrm{FD})]^{-1} \sum_{\mathbf{k}^R \in T^R} \delta^3(\mathbf{k}_1 - \mathbf{k}_1^R)$$
$$\times \exp(i\mathbf{k}_2^R \cdot \mathbf{c}_2) a(\mathbf{k}_1, \mathbf{k}_2); \quad (4.3)$$

where

$$a(\mathbf{k}_1^R, \mathbf{k}_2^R) = \int_{\mathrm{FD}} f(\mathbf{x}_1, \mathbf{x}_2)$$
$$\times \exp[-i(\mathbf{k}_1^R \cdot \mathbf{x}_1 + \mathbf{k}_2^R \cdot \mathbf{x}_2)]\, d^3x_1\, d^3x_2 \quad (4.4)$$

are the Fourier coefficients of the function $f(\mathbf{y}_1, \mathbf{y}_2)$. For the proof see Kramer (1988), proposition 7.1.

Now we choose the 20 *Klötze* of definition 3.3 as the fundamental domain. The Fourier coefficient becomes a first sum over two representatives kl_α and kl_β, and a second sum over the ten representatives of the coset I/D_3:

$$a(\mathbf{k}_1^R, \mathbf{k}_2^R) = \sum_{\xi=\alpha,\beta} \sum_{j=1}^{10} \int_{kl_\xi(3+3; c_j g_\xi)} f_{\xi j}(\mathbf{x}_1, \mathbf{x}_2)$$
$$\times \exp[-i(\mathbf{k}_1^R \cdot \mathbf{x}_1 + \mathbf{k}_2^R \cdot \mathbf{x}_2)]\, d^3x_1\, d^3x_2. \quad (4.5)$$

Here $f_{\xi j}(\mathbf{x}_1, \mathbf{x}_2)$ denotes the density on the *Klotz* with label $\xi = \alpha$ or β and transformed by the coset generator c_j from Table 1. Icosahedral point symmetry requires that the density $f_{\xi j}(\mathbf{x}_1, \mathbf{x}_2)$ on each *Klotz* has D_3 point symmetry with respect to the centre, and that moreover $f_{\xi j}(\mathbf{x}_1, \mathbf{x}_2)$ be independent of the coset label j. This means that there are only two representative *Klötze*, each with D_3 point symmetry, if the full space group (T, I) is considered.

The expression of (4.5) with this space-group restriction is still general. In the quasicrystal model, the density on each *Klotz* is restricted by

$$f_{\xi j}(\mathbf{x}_1, \mathbf{x}_2) = f_{\xi j}(\mathbf{x}_1). \quad (4.6)$$

The restricted density $f_{\xi j}(\mathbf{x}_1)$ can now be associated with the 1-chart of the *Klotz* kl_ξ, that is, with a thin or a thick rhombohedron. Again, this three-dimensional density must have D_3 point symmetry with respect to the centre of the rhombohedron. Independence of the index j implies that the density be fixed to the rhombohedra independent of their orientation in E_1^3. These properties lead to:

4.2. *Proposition*

The Fourier transform of the icosahedral quasicrystal model is given by

$$\tilde{f}(\mathbf{k}_1)=[\text{vol. (FD)}]^{-1}\sum_{\xi=\alpha,\beta}\sum_{j=1}^{10}\tilde{f}_{\xi j}(\mathbf{k}_1)Q_{\xi j}(\mathbf{k}_1) \quad (4.7)$$

where the *structure factor*

$$\tilde{f}_{\xi j}(\mathbf{k}_1)=\int_{h_1^*(3;c_jg_\xi)} f_\xi(\mathbf{x}_1)\exp(-i\mathbf{k}_1\,.\,\mathbf{x}_1)\,\mathrm{d}^3x_1 \quad (4.8)$$

is the Fourier transform of the density on a quasicrystal cell in E_1^3, of orientation given by the action of c_j on the representative kl_α or kl_β. The expression

$$Q_{\xi j}(\mathbf{k}_1)=\sum_{\mathbf{k}^R\in T^R}\delta^3(\mathbf{k}_1-\mathbf{k}_1^R)\exp(i\mathbf{k}_2^R\,.\,\mathbf{c}_2)K_{\xi j}(\mathbf{k}_2^R) \quad (4.9)$$

will be called the *quasilattice factor*, and

$$K_{\xi j}(\mathbf{k}_2^R)=\int_{h_2(3;c_jg_\xi)}\exp(-i\mathbf{k}_2^R\,.\,\mathbf{x}_2)\,\mathrm{d}^3x_2 \quad (4.10)$$

will be called the *kinematical factor.* This kinematical factor is in E_2^3 the Fourier transform of the 2-chart of the *Klotz* labelled by ξ and j. It is independent of the density and is completely determined by the geometry of the *Klötze.*

In deriving proposition 4.2 we used the fact that $\mathbf{k}_1$ and $\mathbf{k}_1^R$ are related by a δ function. The kinematical factors will be computed in § 5. These factors play an important part in damping the Fourier coefficients for large values of $|\mathbf{k}_2^R|$.

If the density $f_{\xi j}(\mathbf{x}_1)$ is concentrated on the boundaries of a rhombohedron, that is, on the vertices, edges or faces, one obtains modified expressions for the Fourier transform which again involve quasilattice factors and kinematical factors. These expressions are computed in § 5.

5. Kinematical factors and their computation

As shown by Kramer (1988), the boundaries of the *Klötze* require a special analysis in view of their different symmetry groups. In this section we compute with respect to the quasicrystal model the kinematical factors for density distributions non-vanishing only on *Klotz* boundaries of fixed dimension. A composition of these density distributions leads to a general density distribution.

We consider the *Klotz* boundaries defined in (3.10) for $p=6, 5, 4$; $p=3$ describes the original *Klotz.* The dual boundary $h^*(6-p;g)$ is projected on E_1^3, the projected *Klotz* boundary $kl_1((6-p)+3;g)$ yields the vertices, edges and faces of the projected *Klötze* $kl_1(3+3;\tilde{g})$ for $p=6, 5, 4$ respectively, whereas in E_2^3 three-dimensional polytopes will be obtained. For $p=6, 5, 4, 3$ the *Klotz* polytopes $kl((6-p)+3;g)$ have the stability groups $St=I, D_5, D_2, D_3$ referred to their centres; the coset generators c_i, c_i', c_i'' of I/St and the group elements $g_\xi\in\Omega(6)$, which determine the representative *Klotz* boundaries, are given in Tables 1 and 5. The full set of boundaries in E^6 is obtained by first acting with the coset generators, then acting with all translations $\mathbf{b}\in T$ on the representatives. In contrast to the case $p=3$, only one representative *Klotz* boundary exists for the cases $p\geq 4$, *i.e.* given a density distribution on a representative *Klotz* boundary, the density on all other *Klotz* boundaries with same dimensionality is fixed by symmetry. For example, at each vertex the same type of atoms must occur. The Fourier transform for a density distribution on a p-boundary is given by

$$\tilde{f}(\mathbf{k}_1)=\sum_{j=1}^{L}\tilde{f}_j^p(\mathbf{k}_1)Q_j^p(\mathbf{k}_1) \quad (5.1)$$

with the *quasilattice factor*

$$Q_j^p(\mathbf{k}_1)=\sum_{\mathbf{k}^R\in T^R}\{\delta^3(\mathbf{k}_1-\mathbf{k}_1^R)\exp(i\mathbf{k}_2^R\,.\,\mathbf{c}_2)K_j^p(\mathbf{k}_2^R)\}. \quad (5.2)$$

Here L is the number of coset generators. The *structure factors* $\tilde{f}_j^p$ and the *kinematical factors* K_j^p are functions of the elements c_jg_α, c_jg_β, $c_j'g_\gamma$ or $c_j''g_\delta$. To compute the structure factors $\tilde{f}_j^p$ we substitute the integral variables by $\lambda_{r(p+1)}\ldots\lambda_{r(6)}$ and consider the density distributions f_j^p as functions of $\lambda_{r(p+1)}\ldots\lambda_{r(6)}$. In Table 6 we give the explicit forms of $\tilde{f}_j^p$ and K_j^p.

The kinematical factor

$$K_j^p(\mathbf{k}_2^R)=\int_{h_2(p;g)}\exp(-i\mathbf{k}_2^R\,.\,\mathbf{x}_2)\,\mathrm{d}^3x_2 \quad (5.3)$$

consists of a three-dimensional integration over the three-dimensional polytopes $h_2(p;g)$. These polytopes in E_2^3 are the 'shadows' of the p-dimensional boundary $h(p;g)$ obtained by projection. As shown by Haase *et al.* (1987) $h_2(p;g)$, $p=6, 5, 4, 3$ are zonohedra with $p(p-1)$ rhombic faces. For $p=6$ we obtain the Kepler triacontahedron with 30 faces and for $p=3$ the two different rhombohedra with six faces.

To compute the kinematical factor we change the volume integral into a surface integral:

$$\int_V \exp(-i\mathbf{k}_2\,.\,\mathbf{x}_2)\,\mathrm{d}^3x_2 = i|\mathbf{k}_2|^{-2}\int_{\partial V}\exp(-i\mathbf{k}_2\,.\,\mathbf{x}_2)(\mathbf{k}_2\,.\,\mathrm{d}\mathbf{f}). \quad (5.4)$$

The surface integral is the sum of $\frac{1}{2}p(p-1)$ integrals over pairs of rhombic faces. With the auxiliary function $L(z)=\sin(z)/z$ the result of the computation is

Table 6. *Structure factors* $\tilde{f}^p_j(\mathbf{k}_1)$ *and kinematical factors* $K^p_j(\mathbf{k}_2)$ *for* $p=6, 5, 4, 3$.

$f(\lambda_{r(p+1)}\ldots\lambda_{r(6)})$ denotes the density distribution defined on the projected representative *Klotz* boundary $kl_1((6-p)+3;\ g_\xi)$. The permutations r are functions of $c'_j g_\gamma$, $c''_j g_\delta$, $c_j g_\alpha$ or $c_j g_\beta$. L is the number of coset generators.

$p=6,\ L=1$

$$f^6(\mathbf{x}_1)=w_6\delta^3(\mathbf{x}_1)$$

$$\tilde{f}^6(\mathbf{k}_1)=w_6$$

$$K^6(\mathbf{k}_2)=\int_{h_2(6)}\exp(-i\mathbf{k}_2\,.\,\mathbf{x}_2)\,\mathrm{d}^3x_2$$

$p=5,\ L=6$

$$f^5_j(\mathbf{x}_1)=f(\lambda_{r(6)})$$

$$\tilde{f}^5_j(\mathbf{k}_1)=\exp(-i\tfrac{1}{2}\mathbf{k}_1\varepsilon_{r(6)}\,.\,\mathbf{b}_{r(6)1})\tfrac{1}{2}|\mathbf{b}_{r(6)1}|\times\int f(\lambda_{r(6)})\exp(-i\tfrac{1}{2}\mathbf{k}_1\lambda_{r(6)}\varepsilon_{r(6)}\,.\,\mathbf{b}_{r(6)1})\,\mathrm{d}\lambda_{r(6)}$$

$$K^5_j(\mathbf{k}_2)=\int_{h_2(5;c'_jg_\gamma)}\exp(-i\mathbf{k}_2\,.\,\mathbf{x}_2)\,\mathrm{d}^3x_2$$

$p=4,\ L=15$

$$f^4_j(\mathbf{x}_1)=f(\lambda_{r(5)}\lambda_{r(6)})$$

$$\tilde{f}^4_j(\mathbf{k}_1)=\exp\left(-i\tfrac{1}{2}\mathbf{k}_1\,.\sum_{i=5}^{6}\varepsilon_{r(i)}\mathbf{b}_{r(i)1}\right)(\tfrac{1}{2})^2|\mathbf{b}_{r(5)1}\times\mathbf{b}_{r(6)1}|\times\int f(\lambda_{r(5)}\lambda_{r(6)})\exp\left(-i\tfrac{1}{2}\mathbf{k}_1\,.\sum_{i=5}^{6}\lambda_{r(i)}\varepsilon_{r(i)}\mathbf{b}_{r(i)1}\right)\mathrm{d}\lambda_{r(5)}\,\mathrm{d}\lambda_{r(6)}$$

$$K^4_j(\mathbf{k}_2)=\int_{h_2(4;c''_jg_\delta)}\exp(-i\mathbf{k}_2\,.\,\mathbf{x}_2)\,\mathrm{d}^3x_2$$

$p=3,\ L=10$

$$f^3_j(\mathbf{x}_1)=\sum_{\xi=\alpha,\beta}f_\xi(\lambda_{r(4)}\lambda_{r(5)}\lambda_{r(6)})$$

$$\tilde{f}^3_j(\mathbf{k}_1)=\sum_{\xi=\alpha,\beta}\left\{\exp\left(-i\tfrac{1}{2}\mathbf{k}_1\,.\sum_{i=4}^{6}\varepsilon_{r(i)}\mathbf{b}_{r(i)1}\right)(\tfrac{1}{2})^3\times|\det(\mathbf{b}_{r(4)1}\mathbf{b}_{r(5)1}\mathbf{b}_{r(6)1})|\int f_\xi(\lambda_{r(4)}\lambda_{r(5)}\lambda_{r(6)})\times\exp\left(-i\tfrac{1}{2}\mathbf{k}_1\,.\sum_{i=4}^{6}\lambda_{r(i)}\varepsilon_{r(i)}\mathbf{b}_{r(i)1}\right)\mathrm{d}\lambda_{r(4)}\,\mathrm{d}\lambda_{r(5)}\,\mathrm{d}\lambda_{r(6)}\right\}$$

$$K^3_j(\mathbf{k}_2)=\int_{h_2(4;c_jg_\alpha)}\exp(-i\mathbf{k}_2\,.\,\mathbf{x}_2)\,\mathrm{d}^3x_2+\int_{h_2(4;c_jg_\beta)}\exp(-i\mathbf{k}_2\,.\,\mathbf{x}_2)\,\mathrm{d}^3x_2.$$

given by

$$\begin{aligned}\int_{h_2(p,g)}\exp(-i\mathbf{k}_2\,.\,\mathbf{x}_2)\,\mathrm{d}^3x_2&=\exp\left(-i\,\tfrac{1}{2}k_2\,.\sum_{j=p+1}^{6}\varepsilon_{r(j)}\mathbf{b}_{r(j)2}\right)\\&\quad\times2|\mathbf{k}_2|^{-2}\sum_{i<j}^{p}\{[\mathbf{k}_2\,.\,(\mathbf{b}_{r(i)2}\times\mathbf{b}_{r(j)2})]\\&\quad\times(\mathbf{k}_2\,.\,\mathbf{q}_{r(i)r(j)})L(\tfrac{1}{2}\mathbf{k}_2\,.\,\mathbf{b}_{r(i)2})\\&\quad\times L(\tfrac{1}{2}\mathbf{k}_2\,.\,\mathbf{b}_{r(j)2})L(\mathbf{k}_2\,.\,\mathbf{q}_{r(i)r(j)})\}\end{aligned}\qquad(5.5)$$

for $p=3, 4, 5, 6$. The vector $\mathbf{q}_{ij}$ labels the centre of the zonohedral face spanned by the vectors $\mathbf{b}_{i2}$ and $\mathbf{b}_{j2}$. It is defined by

$$\mathbf{q}_{ij}=\tfrac{1}{2}\sum_{l=1,l\neq i,j}^{p}\operatorname{sign}[\mathbf{b}_{l2}\,.\,(\mathbf{b}_{i2}\times\mathbf{b}_{j2})]\mathbf{b}_{l2}.\qquad(5.6)$$

Note that for increasing $|\mathbf{k}_2|$ the product of the three functions L yields a decrease of the amplitude of the kinematical factor to a value smaller than any given value $m>0$.

6. Examples: point scatterers in quasicrystals

The analytical form of the Fourier transform given in (5.1) allows a computation of diffraction patterns of quasicrystals. In the Born approximation the scattered intensity in a direction defined by a wave vector $\mathbf{k}$ is proportional to $|\tilde{f}(\mathbf{k}-\mathbf{k}^0)|^2$, $\mathbf{k}^0$ denotes the wave vector of the incident wave ($\mathbf{k}^0,\mathbf{k}\in E^3_1$). If elastic scattering is assumed ($|\mathbf{k}|=|\mathbf{k}^0|$) and if $|\mathbf{k}^0|$ is large compared to reciprocal-lattice distances (*i.e.* for an incident beam of high energy) the diffraction pattern is determined by those wave vectors $\mathbf{k}$ which lie in the Ewald plane defined by its normal vector $\mathbf{k}^0$. To compute $|\tilde{f}(\mathbf{k}_1)|^2$ we replace $\delta^3(\mathbf{k}_1-\mathbf{k}^R_{i1})\,.\,\delta^3(\mathbf{k}_1-\mathbf{k}^R_{j1})$ by $\delta_{ij}\,.\,\delta^3(\mathbf{k}_1-\mathbf{k}^R_{j1})$, *i.e.* the δ functions are approximations of functions with very small half-widths.

The projected reciprocal-lattice vectors $\mathbf{k}^R_1$ lie dense in E^3_1; thus in a finite area of the Ewald plane there exists an infinite number of projected vectors $\mathbf{k}^R_1$. Restriction to reciprocal-lattice vectors $|\mathbf{k}^R|$ with $|\mathbf{k}^R_2|<k_{2\max}$ leads to a finite number of $\mathbf{k}^R_1$ in a finite area of the Ewald plane. Since the kinematical factor becomes small for large $|\mathbf{k}_2|$, for an appropriate choice of $k_{2\max}$ no vector $\mathbf{k}^R$ with intensity larger than a given minimal intensity will be excluded. The restriction discussed amounts to neglecting reciprocal-lattice vectors $\mathbf{k}^R$ with intensities smaller than the given minimal intensity.

We choose the incident wave vector $\mathbf{k}^0$ parallel to a fivefold axis of the quasilattice: $\mathbf{k}^0\propto\mathbf{b}_{11}$. The conditions

$$\begin{aligned}&(a)\ \ \mathbf{k}^R_1\,.\,\mathbf{b}_{11}=0\\&(b)\ \ |\mathbf{k}^R_1|<10\times2\pi\\&(c)\ \ |\mathbf{k}^R_2|<k_{2\max}=20\end{aligned}\qquad(6.1)$$

yield a finite set of vectors $\mathbf{k}^R$ in E^6. Conditions (a) and (b) select a circle with radius $10\times2\pi$ on the Ewald plane in E^3_1, condition (c) excludes vectors with negligible intensity. The value of $k_{2\max}$ is estimated by setting the minimal intensity equal to 1% of the maximal intensity defined by $|\tilde{f}(\mathbf{k}_1=0)|^2$.

The density distributions on the *Klotz* boundaries are chosen as point scatterers defined by δ functions. The point scatterers are placed into the centres of the boundaries:

$$f(\mathbf{x}_1)=w_p\delta^3(\mathbf{x}_1);\qquad p=6$$

$$f(\lambda_{r(p+1)}\ldots\lambda_{r(6)})=w_p\delta^{6-p}(\lambda_{r(p+1)}\ldots\lambda_{r(6)});\qquad(6.2)$$

$$p=5,4,3.$$

Hence the structure factors are given by

$$\tilde{f}^{p=6}(\mathbf{k}_1)=w_p;\qquad p=6$$

$$\tilde{f}^{p}(\mathbf{k}_1)=w_p\exp\left(-i\tfrac{1}{2}\mathbf{k}_1\,.\sum_{j=p+1}^{6}\varepsilon_{r(j)}\mathbf{b}_{r(j)1}\right)\times(\tfrac{1}{2})^{(p-6)}V(p);\qquad p=5,4,3.\qquad(6.3)$$

$V(p)$ gives the $(6-p)$-dimensional volume spanned by the vectors $\mathbf{b}_{r(p+1)1}\ldots\mathbf{b}_{r(6)1}$ in E_1^3. We determine the weight factors w_p by the conditions

$$\tilde{f}^p(\mathbf{k}_1=0)=1, \quad p=6,5,4,3. \tag{6.4}$$

In Figs. 3(a)–(f) we give some results of the computed diffraction patterns. The fivefold symmetry together with the inversion symmetry caused by Friedel's law lead to a tenfold symmetry of $|\tilde{f}(\mathbf{k}_1)|^2$. Therefore in Figs. 3($a$)–($f$) only one sector with aperture angle 36° is shown. The vectors $\mathbf{k}^R$ are labelled by six Miller indices $h_1\ldots h_6$ defined by $\mathbf{k}^R=2\pi\sum_{i=1}^6 h_i\mathbf{b}_i$. In

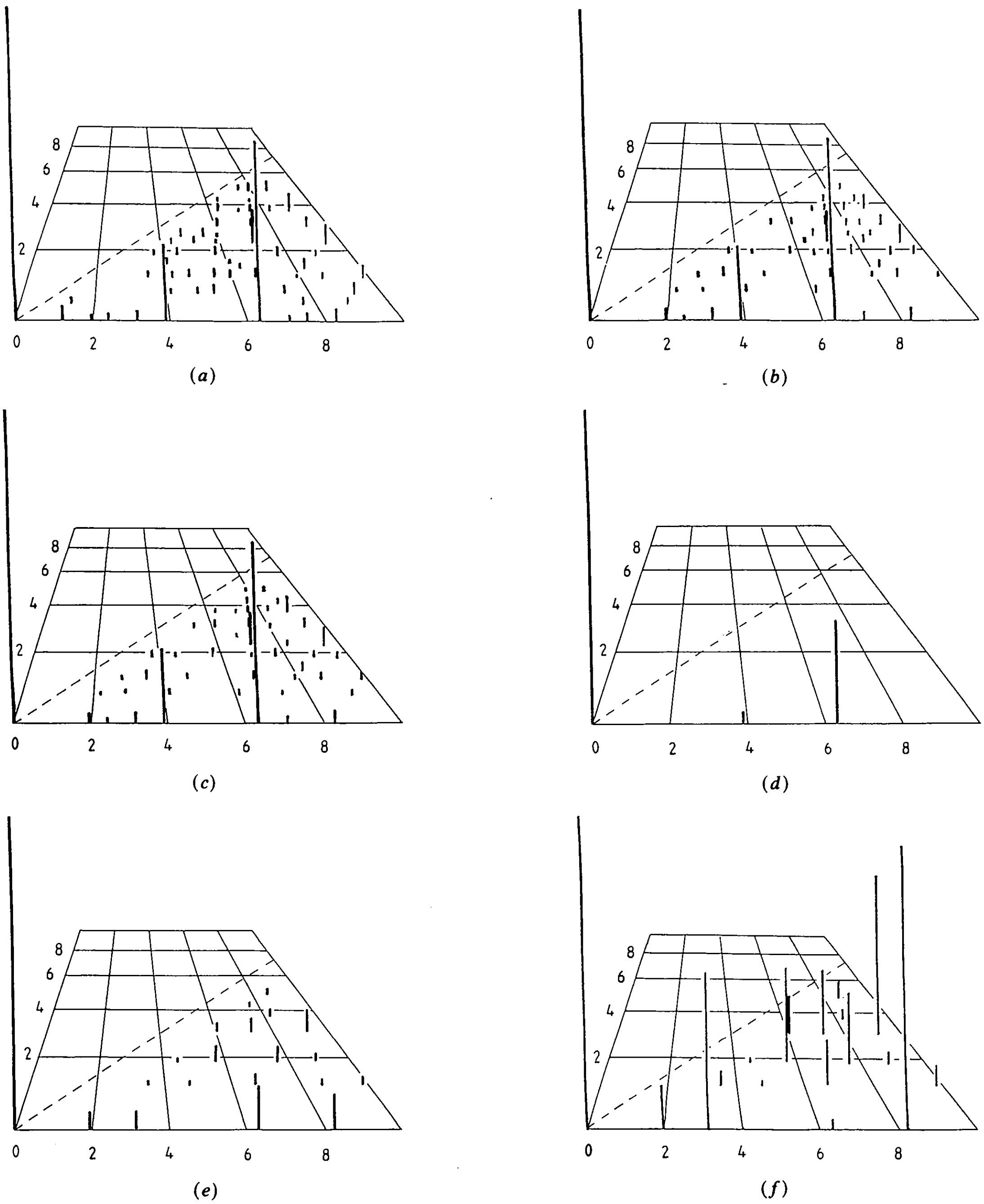

Fig. 3. Intensity of diffraction, represented by vertical bars, in a section of a plane perpendicular to a fivefold axis. The numbers in the plane mark multiples of 2π. Point-like atoms are assumed (a) at the centres of all thin rhombohedra ($p=3$); (b) at the centres of all thick rhombohedra ($p=3$); (c) at the centres of all thick and all thin rhombohedra ($p=3$); (d) at the centres of the faces of all rhombohedral cells ($p=4$); (e) at the centres of the edges of all rhombohedral cells ($p=5$); and (f) at the vertices of all rhombohedral cells ($p=6$).

Table 7. *Miller indices $h_1 \ldots h_6$, intensities and coordinates of the diffraction peaks* (*cf.* Fig. 3)

The abscissa is parallel to $(\mathbf{b}_5 - \mathbf{b}_2)_1$, the ordinate is perpendicular to the abscissa. Table 7(*a*) corresponds to Fig. 3(*a*), Table 7(*b*) to Fig. 3(*b*) *etc.*

(*a*) $p=3$, thin rhombohedra occupied, thick rhombohedra vacant

h_1	h_2	h_3	h_4	h_5	h_6	Int.	Absc.	Ord.
0	0	0	0	0	0	1·000	0·00	0·00
0	−1	0	0	1	0	0·046	1·20	0·00
0	−1	−1	1	1	0	0·019	1·95	0·00
0	−2	0	0	2	0	0·022	2·41	0·00
0	−2	−1	1	2	0	0·032	3·15	0·00
0	−2	−2	2	2	0	0·240	3·89	0·00
0	−3	−1	2	2	0	0·012	4·12	0·71
0	−3	−2	3	2	0	0·014	4·87	0·71
0	−3	−2	2	3	0	0·041	5·10	0·00
0	−4	−1	2	3	0	0·027	5·33	0·71
0	−4	−2	2	4	0	0·585	6·30	0·00
0	−4	−3	3	4	0	0·012	7·04	0·00
0	−5	−1	3	3	0	0·012	6·30	1·41
0	−5	−2	3	4	0	0·024	7·27	0·71
0	−5	−2	2	5	0	0·026	7·50	0·00
0	−5	−3	3	5	0	0·039	8·25	0·00
0	−5	−4	4	5	0	0·037	8·99	0·00
0	−6	−2	4	4	0	0·032	8·25	1·41
0	−6	−3	4	5	0	0·037	9·22	0·71
0	0	−1	1	1	−1	0·015	1·34	0·44
0	−2	−1	2	2	−1	0·017	3·52	1·14
0	−2	−2	3	2	−1	0·012	4·27	1·14
0	−3	0	2	2	−1	0·012	3·75	1·85
0	−3	−1	3	2	−1	0·030	4·49	1·85
0	−3	−1	2	3	−1	0·030	4·72	1·14
0	−3	−2	3	3	−1	0·030	5·47	1·14
0	−4	0	3	2	−1	0·027	4·72	2·56
0	−4	−1	4	2	−1	0·027	5·47	2·56
0	−4	−1	3	3	−1	0·039	5·70	1·85
0	−4	−1	2	4	−1	0·027	5·93	1·14
0	−4	−2	3	4	−1	0·032	6·67	1·14
0	−4	−3	3	5	−1	0·018	7·64	0·44
0	−5	0	3	3	−1	0·012	5·93	2·56
0	−5	−2	4	4	−1	0·029	7·64	1·85
0	−5	−2	3	5	−1	0·011	7·87	1·14
0	−5	−3	4	5	−1	0·013	8·62	1·14
0	−5	−3	3	6	−1	0·020	8·85	0·44
0	−6	−2	4	5	−1	0·021	8·85	1·85
0	−6	−3	4	6	−1	0·040	9·82	1·14
0	−2	−1	2	3	−2	0·012	4·12	1·58
0	−3	0	2	3	−2	0·014	4·35	2·29
0	−3	−1	3	3	−2	0·030	5·10	2·29
0	−3	−2	4	3	−2	0·010	5·84	2·29
0	−3	−2	3	4	−2	0·010	6·07	1·58
0	−4	−1	4	3	−2	0·032	6·07	3·00
0	−4	−2	4	4	−2	0·137	7·04	2·29
0	−5	0	4	3	−2	0·024	6·30	3·70
0	−5	−1	5	3	−2	0·011	7·04	3·70
0	−5	−1	4	4	−2	0·029	7·27	3·00
0	−6	0	4	4	−2	0·032	7·50	3·70
0	−6	−1	5	4	−2	0·021	8·25	3·70
0	−6	−2	6	4	−2	0·078	8·99	3·70
0	−6	−2	5	5	−2	0·037	9·22	3·00
0	−6	−2	4	6	−2	0·078	9·45	2·29
0	−4	−1	5	3	−3	0·018	6·44	4·14
0	−5	−1	6	3	−3	0·020	7·42	4·85
0	−5	−1	5	4	−3	0·013	7·64	4·14
0	−6	0	5	4	−3	0·037	7·87	4·85
0	−6	−1	6	4	−3	0·040	8·62	4·85

(*b*) $p=3$, thin rhombohedra vacant, thick rhombohedra occupied

h_1	h_2	h_3	h_4	h_5	h_6	Int.	Absc.	Ord.
0	0	0	0	0	0	1·000	0·00	0·00
0	−1	−1	1	1	0	0·037	1·95	0·00
0	−2	0	1	1	0	0·013	2·18	0·71
0	−2	−1	2	1	0	0·012	2·92	0·71
0	−2	0	0	2	0	0·013	2·41	0·00
0	−2	−1	1	2	0	0·037	3·15	0·00
0	−2	−2	2	2	0	0·237	3·89	0·00
0	−3	−1	2	2	0	0·024	4·12	0·71
0	−3	−1	1	3	0	0·019	4·35	0·00
0	−3	−2	2	3	0	0·035	5·10	0·00
0	−4	−2	3	3	0	0·020	6·07	0·71
0	−4	−2	2	4	0	0·584	6·30	0·00
0	−4	−3	3	4	0	0·026	7·04	0·00
0	−5	−3	3	5	0	0·040	8·25	0·00
0	−6	−2	4	4	0	0·022	8·25	1·41
0	−6	−3	3	6	0	0·016	9·45	0·00
0	−2	0	1	2	−1	0·012	2·78	1·14
0	−2	−1	2	2	−1	0·033	3·52	1·14
0	−3	0	2	2	−1	0·024	3·75	1·85
0	−3	−1	3	2	−1	0·015	4·49	1·85
0	−3	−1	2	3	−1	0·015	4·72	1·14
0	−4	−1	3	3	−1	0·028	5·70	1·85
0	−4	−2	4	3	−1	0·012	6·44	1·85
0	−4	−2	3	4	−1	0·027	6·67	1·14
0	−5	−1	4	3	−1	0·017	6·67	2·56
0	−5	−1	3	4	−1	0·017	6·90	1·85
0	−5	−2	4	4	−1	0·034	7·64	1·85
0	−5	−2	3	5	−1	0·014	7·87	1·14
0	−5	−3	4	5	−1	0·025	8·62	1·14
0	−6	−1	4	4	−1	0·012	7·87	2·56
0	−6	−2	5	4	−1	0·015	8·62	2·56
0	−6	−2	4	5	−1	0·027	8·85	1·85
0	−6	−3	5	5	−1	0·027	9·59	1·85
0	−6	−3	4	6	−1	0·016	9·82	1·14
0	−4	0	3	3	−2	0·020	5·33	3·00
0	−4	−1	4	3	−2	0·027	6·07	3·00
0	−4	−1	3	4	−2	0·012	6·30	2·29
0	−4	−2	4	4	−2	0·131	7·04	2·29
0	−5	−1	5	3	−2	0·014	7·04	3·70
0	−5	−1	4	4	−2	0·034	7·27	3·00
0	−5	−2	5	4	−2	0·022	8·02	3·00
0	−5	−2	4	5	−2	0·022	8·25	2·29
0	−6	0	4	4	−2	0·022	7·50	3·70
0	−6	−1	5	4	−2	0·027	8·25	3·70
0	−6	−2	6	4	−2	0·070	8·99	3·70
0	−6	−1	4	5	−2	0·015	8·48	3·00
0	−6	−2	5	5	−2	0·038	9·22	3·00
0	−6	−2	4	6	−2	0·070	9·45	2·29
0	−5	−1	5	4	−3	0·025	7·64	4·14
0	−6	−1	6	4	−3	0·016	8·62	4·85
0	−6	−1	5	5	−3	0·027	8·85	4·14

(*c*) $p=3$, thin rhombohedra and thick rhombohedra occupied

h_1	h_2	h_3	h_4	h_5	h_6	Int.	Absc.	Ord.
0	0	0	0	0	0	1·000	0·00	0·00
0	−1	−1	1	1	0	0·032	1·95	0·00
0	−2	0	1	1	0	0·011	2·18	0·71
0	−2	−1	2	1	0	0·010	2·92	0·71
0	−2	0	0	2	0	0·016	2·41	0·00
0	−2	−1	1	2	0	0·036	3·15	0·00
0	−2	−2	2	2	0	0·238	3·89	0·00
0	−3	−1	2	2	0	0·021	4·12	0·71
0	−3	−2	2	3	0	0·037	5·10	0·00
0	−4	−2	3	3	0	0·015	6·07	0·71
0	−4	−2	2	4	0	0·585	6·30	0·00
0	−4	−3	3	4	0	0·022	7·04	0·00
0	−5	−2	3	4	0	0·013	7·27	0·71
0	−5	−3	3	5	0	0·039	8·25	0·00
0	−6	−2	4	4	0	0·025	8·25	1·41
0	−6	−3	4	5	0	0·012	9·22	0·71
0	−6	−3	3	6	0	0·011	9·45	0·00
0	−2	0	1	2	−1	0·010	2·78	1·14
0	−2	−1	2	2	−1	0·028	3·52	1·14
0	−3	0	2	2	−1	0·021	3·75	1·85
0	−3	−1	3	2	−1	0·019	4·49	1·85
0	−3	−1	2	3	−1	0·019	4·72	1·14
0	−4	−1	3	3	−1	0·031	5·70	1·85
0	−4	−2	3	4	−1	0·028	6·67	1·14
0	−5	−1	4	3	−1	0·010	6·67	2·56
0	−5	−1	3	4	−1	0·010	6·90	1·85
0	−5	−2	4	4	−1	0·033	7·64	1·85
0	−5	−2	3	5	−1	0·013	7·87	1·14
0	−5	−3	4	5	−1	0·022	8·62	1·14

Table 7 (*cont.*)

h_1	h_2	h_3	h_4	h_5	h_6	Int.	Absc.	Ord.
(*c*) $p=3$ (*cont.*)								
0	−6	−2	4	5	−1	0·025	8·85	1·85
0	−6	−3	5	5	−1	0·019	9·59	1·85
0	−6	−3	4	6	−1	0·021	9·82	1·14
0	−4	0	3	3	−2	0·015	5·33	3·00
0	−4	−1	4	3	−2	0·028	6·07	3·00
0	−4	−2	4	4	−2	0·133	7·04	2·29
0	−5	0	4	3	−2	0·013	6·30	3·70
0	−5	−1	5	3	−2	0·013	7·04	3·70
0	−5	−1	4	4	−2	0·033	7·27	3·00
0	−5	−2	5	4	−2	0·015	8·02	3·00
0	−5	−2	4	5	−2	0·015	8·25	2·29
0	−6	0	4	4	−2	0·025	7·50	3·70
0	−6	−1	5	4	−2	0·025	8·25	3·70
0	−6	−2	6	4	−2	0·072	8·99	3·70
0	−6	−2	5	5	−2	0·038	9·22	3·00
0	−6	−2	4	6	−2	0·072	9·45	2·29
0	−5	−1	5	4	−3	0·022	7·64	4·14
0	−6	0	5	4	−3	0·012	7·87	4·85
0	−6	−1	6	4	−3	0·021	8·62	4·85
0	−6	−1	5	5	−3	0·019	8·85	4·14
(*d*) $p=4$								
0	0	0	0	0	0	1·000	0·00	0·00
0	−2	−2	2	2	0	0·033	3·89	0·00
0	−4	−2	2	4	0	0·324	6·30	0·00
(*e*) $p=5$								
0	0	0	0	0	0	1·000	0·00	0·00
0	−1	−1	1	1	0	0·052	1·95	0·00
0	−2	−1	1	2	0	0·055	3·15	0·00
0	−2	−1	2	2	−1	0·012	3·52	1·14
0	−3	−1	2	3	−1	0·011	4·72	1·14
0	−3	−1	3	2	−1	0·011	4·49	1·85
0	−4	−1	3	3	−1	0·055	5·70	1·85
(*e*) $p=5$ (*cont.*)								
0	−4	−1	4	3	−2	0·031	6·07	3·00
0	−5	−1	4	4	−2	0·056	7·27	3·00
0	−5	−1	5	4	−3	0·014	7·64	4·14
0	−6	−1	5	4	−2	0·029	8·25	3·70
0	−6	−1	6	4	−3	0·025	8·62	4·85
0	−3	−2	2	3	0	0·095	5·10	0·00
0	−4	−2	2	4	0	0·133	6·30	0·00
0	−4	−2	3	4	−1	0·031	6·67	1·14
0	−5	−2	4	4	−1	0·056	7·64	1·85
0	−6	−2	4	5	−1	0·029	8·85	1·85
0	−6	−2	5	5	−2	0·095	9·22	3·00
0	−5	−3	3	5	0	0·107	8·25	0·00
0	−5	−3	4	5	−1	0·014	8·62	1·14
0	−6	−3	4	6	−1	0·025	9·82	1·14
(*f*) $p=6$								
0	0	0	0	0	0	1·000	0·00	0·00
0	−1	−1	1	1	0	0·135	1·95	0·00
0	−2	−1	1	2	0	0·502	3·15	0·00
0	−3	−2	2	3	0	0·775	5·10	0·00
0	−4	−2	2	4	0	0·031	6·30	0·00
0	−5	−3	3	5	0	0·908	8·25	0·00
0	−2	−1	2	2	−1	0·049	3·52	1·14
0	−3	−1	3	2	−1	0·013	4·49	1·85
0	−3	−1	2	3	−1	0·013	4·72	1·14
0	−4	−1	3	3	−1	0·377	5·70	1·85
0	−4	−2	3	4	−1	0·167	6·67	1·14
0	−5	−2	4	4	−1	0·280	7·64	1·85
0	−6	−2	4	5	−1	0·041	8·85	1·85
0	−6	−3	4	6	−1	0·081	9·82	1·14
0	−4	−1	4	3	−2	0·167	6·07	3·00
0	−5	−1	4	4	−2	0·280	7·27	3·00
0	−6	−1	5	4	−2	0·041	8·25	3·70
0	−6	−2	5	5	−2	0·701	9·22	3·00
0	−6	−1	6	4	−3	0·081	8·62	4·85

Tables 7(a)–(f) we give the indices of the diffraction peaks.

By comparing the different diffraction patterns notice that the weight factors w_p are not identical. Nevertheless note the qualitative differences of Figs. 3(a)–(f). As in periodic crystallography, the position of the diffraction peaks is determined by the quasilattice, whereas the intensity of the peaks depends on the density distribution.

References

Bohr, H. (1925*a*). *Acta Math.* **45**, 29–127.

Bohr, H. (1925*b*). *Acta Math.* **46**, 101–214.

Bohr, H. (1926). *Acta Math.* **47**, 237–281.

Coxeter, H. S. M. & Moser, W. O. (1965). *Generators and Relations for Discrete Groups*, pp. 88–92. Berlin: Springer.

Haase, R. W., Kramer, L., Kramer, P. & Lalvani, H. (1987). *Acta Cryst.* A**43**, 574–587.

Hahn, Th. & Klapper, H. (1983). *Point Groups and Crystal Classes.* In *International Tables for Crystallography*, Vol. A. *Space-Group Symmetry*, edited by Th. Hahn, pp. 745–786. Dordrecht: Reidel. (Present distributor Kluwer Academic Publishers, Dordrecht.)

Kramer, P. (1987). *Acta Cryst.* A**43**, 486–489.

Kramer, P. (1988). *J. Math. Phys.* **29**, 516–524.

Kramer, P. (1989). Submitted.

Kramer, P. & Haase, R. W. (1988). *Group Theory of Icosahedral Quasicrystals.* In *Aperiodic Crystals*, edited by M. V. Jaric. New York: Academic Press.

Kramer, P. & Neri, R. (1984). *Acta Cryst.* A**40**, 580–587.

Mackay, A. L. (1982). *Physica* (*Utrecht*), **114**A, 609–613.

Munkres, J. R. (1984). *Elements of Algebraic Topology.* Menlo Park: Addision-Wesley.